Pergamon

Available online at www.sciencedirect.com
SCIENCE DIRECT

Ocean Engineering 30 (2003) 579–599

OCEAN ENGINEERING

www.elsevier.com/locate/oceaneng

Validation of the three-wave quasi-kinetic approximation for the spectral evolution in shallow water

R. Piscopia [a,*], V. Polnikov [b], P. DeGirolamo [c], S. Magnaldi [a]

[a] *DITS Department, University of Rome La Sapienza, Via Eudossiana 18, 00184 Rome, Italy*
[b] *State Oceanographic Institute, Kropotkinskii 6, Moscow, 119838 Russia*
[c] *DISAT Department, University of L'Aquila, Monteluco di Roio, 67040 L'Aquila, Italy*

Received 18 December 2001; accepted 2 May 2002

Abstract

This paper aims at validating the three-wave quasi-kinetic approximation for the spectral evolution of weakly nonlinear gravity waves in shallow water. The problem is investigated using a one-dimensional numerical wave propagation model, formulated in the spectral representation. This model includes both a nonlinear triad interactions term and a wave breaking dissipation term. Some numerical tests were carried out in order to show the importance of using the triad nonlinear term in wave propagation spectral models, particularly to describe both behavior of the spectral integral parameters and of the spectral shape evolution in shallow water depth. Furthermore; a comparison against different set of experimental observations was carried out. Comparing the numerical results with the experimental observations made it possible to show the modeling efficiency of the three-wave quasi-kinetic approximation.

Keywords: Spectral model; Nonlinear wave interaction; Shallow water waves; Wave spectrum evolution

1. Introduction

Numerical modeling of wind waves evolution in coastal zone is important for many practical aims. Furthermore, being related to a correct description of nonlinear

* Corresponding author. Tel.: +39 0644585063; fax: +39 0644585064.
E-mail address: rodolfo.piscopia@uniroma1.it (R. Piscopia).

PII: S0029-8018(02)00058-6

wave interactions during the propagation into shallow water, makes this problem interesting from a scientific point of view.

The nonlinear four-wave interactions play a very important role in gravity wave spectrum evolution (Hasselmann, 1962; Hasselmann et al., 1976; Young and Van Vladder, 1993). Nevertheless, the limit of validity of the four-wave interactions mechanism was not clear until Zaslavskii et al. (1995) investigated on it both analytically and numerically.

As known, the kinetic equation derivation is based on the assumption that in deep water the non-resonant three-wave interactions do not directly contribute to the energy transfer. The contribution of triad interactions can be therefore rearranged in the derivation of the four-wave kinetic equation by considering slow time scale for quadratic terms in the dynamic equations (Zakharov, 1974; Crawford et al., 1980). This assumption is valid for small values of nonlinearity parameter in deep water (i.e. $\epsilon = k_p a \ll 1$, where k_p is the spectral peak wave number and a is the mean wave amplitude).

Zaslavskii et al. (1995) showed that the non-resonant three-wave interactions have an increasing role as the local depth decreases. Furthermore, these authors found that the technique generally used to derive the four-wave kinetic equation does not apply to small values of the relative depth parameter (i.e. $k_p h < 1$, where h is the local depth). The ordinary four-wave kinetic equation is therefore valid in rather deep water only ($k_p h > 1$).

This result was confirmed later by Zakharov (1998) on the basis of different theoretical considerations. Calculating the wave–wave interaction time in shallow water ($k_p h < 1$) and comparing it to the mean wave period, this author found an inconsistency of the time scale method used in the theoretical derivation of the kinetic equation, i.e. the hypothesis of slow time scale for the wave–wave interactions is violated. Thus, the theoretical problem is to find a more correct representation of the nonlinear mechanism responsible for the wave spectrum evolution in shallow water.

Many attempts have been made to give a proper description of the nonlinear evolution mechanism in shallow water using the three-wave interactions. Worthy of note are the pioneer papers of Phillips (1960) and Peregrine (1967), and the more sophisticated approaches of Freilich and Guza (1984); Elgar and Guza (1986); Resio (1988); Madsen and Sørensen (1992, 1993); Abreu et al. (1992); Holthuijensen et al. (1993); Nwogu (1994); Eldeberky and Battjes (1996); Beji and Nadaoka (1997, 1999) and many others. All these approaches give acceptable results. Particularly interesting are those obtained by Eldeberky and Battjes (1996) and Beji and Nadaoka (1999). These authors found good agreement between their numerical simulations and measurements reported by Beji and Battjes (1993). Nevertheless, these last models are not directly spectral models.

A complete spectral representation for the triad-interactions description was firstly derived by Zaslavskii and Polnikov (1998) and then tested by Polnikov (1998), using the concept of finite interaction time. The specific feature of this approach is the appearance of two equations instead of the single traditional kinetic equation. For this reason, the derived theory was named ‘three-wave quasi-kinetic approximation’ for the wave spectrum evolution in shallow water.

As is known, the main theoretical problem is to overcome the difficulty with the non-resonant interactions description. Actually, any three gravity waves cannot meet joint resonant conditions of the kind:

$$\mathbf{k}_1 + \mathbf{k}_2 = \mathbf{k}_3, \tag{1}$$

$$\sigma(k_1) + \sigma(k_2) = \sigma(k_3), \tag{2}$$

where $\mathbf{k}_i$ is the wave number vector of one interacting wave and $\sigma(k_i)$ is the wave angular frequency (hereinafter indicated as frequency for simplicity). The wave number $k = |\mathbf{k}|$ is related to frequency by the dispersion relation, which in absence of current fields has the following expression

$$\sigma^2(k) = gk\tanh(kh), \tag{3}$$

where g is the gravity acceleration. In shallow water, when the value of the relative depth parameter is small ($kh < 1$), $\sigma(k)$ can be approximated as follows:

$$\sigma(k) = (gk)^{1/2}k[1-(kh)^2/6]. \tag{4}$$

In this case, when condition (1) is met, the mismatch in the frequency resonance condition (2) becomes rather small, and the quasi-resonant approximation can therefore be introduced. Section 2 provides a short introduction to the theory, whereas the details can be found in Zaslavskii and Polnikov (1998) and in the bibliography referenced therein.

The main aim of the present paper is the numerical validation of the three-wave quasi-kinetic approximation. The equations of the theory have therefore been introduced into a one-dimensional wave propagation spectral model which is also able to reproduce the effect of wave energy dissipation due to breaking. The set-up numerical model is described in section 3 and the method of investigation is outlined in section 4. Two numerical tests were carried out in order to show the importance of using the three-wave nonlinear term in wave propagation spectral models, particularly to describe both behavior of the integral parameters and the wave spectrum evolution in shallow water depth. Testing results are described and analyzed in section 5. Validation of the numerical results with two different set of experimental observations (Beji and Battjes, 1993; Arcilla et al., 1994) is described and analyzed in section 6. In section 7 the conclusions are drawn.

Finally, the obtained results show clearly that the triad nonlinear interactions are responsible for the wave energy transfer from the fundamental harmonic to the superharmonics. In terms of spectral-integral characteristics, the nonlinearity is responsible for a significant decrease in the mean wave period T_m. Herewith, this decrease is generally not accompanied by a significant change in the root mean square wave height. But, when breaking occurs, the nonlinear interactions increase the energy dissipation rate, transferring energy from long non breaking wave trough short breaking wave. This energy transfer trough the spectral components is very important in describing sediment transport occurring in the near-shore zone.

2. Three-wave Quasi-kinetic approximation for triad interactions

To derive a spectral evolution equation for weak nonlinear waves in shallow water depth with no ambient current field, Zaslavskii and Polnikov (1998) started from the following expression of the Hamilton equation (Zakharov, 1974):

$$\frac{\partial b(\mathbf{k})}{\partial t} + j\sigma(k)b(\mathbf{k}) = -j\int d\mathbf{k}_1\int V_1(\mathbf{k},\mathbf{k}_1,\mathbf{k}_2)b(\mathbf{k}_1)b(\mathbf{k}_2)\delta(\mathbf{k} - \mathbf{k}_1-\mathbf{k}_2)d\mathbf{k}_2$$
$$-j\int d\mathbf{k}_1\int V_2(\mathbf{k},\mathbf{k}_1,\mathbf{k}_2)b^*(\mathbf{k}_1)b(\mathbf{k}_2)\delta(\mathbf{k} + \mathbf{k}_1-\mathbf{k}_2)d\mathbf{k}_2$$
$$-j\int d\mathbf{k}_1\int V_3(\mathbf{k},\mathbf{k}_1,\mathbf{k}_2)b^*(\mathbf{k}_1)b^*(\mathbf{k}_2)\delta(\mathbf{k} + \mathbf{k}_1 + \mathbf{k}_2)d\mathbf{k}_2 +$$
$$-j\int d\mathbf{k}_1\int d\mathbf{k}_2\int W_4(\mathbf{k},\mathbf{k}_1,\mathbf{k}_2,\mathbf{k}_3)b^*(\mathbf{k})b(\mathbf{k}_2)b(\mathbf{k}_3)\delta(\mathbf{k} + \mathbf{k}_1-\mathbf{k}_2-\mathbf{k}_3)d\mathbf{k}_3\} + ... \tag{5}$$

where j is the complex unity, star ($*$) stands for the complex conjugate, $V_1(...)$, $V_2(...)$ and $V_3(\ldots)$ are the three-wave interaction coefficients, $W_4(...)$ is the most important four-wave interaction coefficient, $\delta(\ldots)$ is the Dirac's delta-function and

$$b(\mathbf{k}) = \sqrt{\frac{\sigma(k)}{2g}}\zeta(\mathbf{k}) + j\sqrt{\frac{g}{2\sigma(k)}}\varphi_s(\mathbf{k}) \tag{6}$$

is the 'normal canonical' variable, related to the Fourier-components of both the surface elevation $\zeta(\mathbf{k})$ and the surface velocity potential $\phi_s(\mathbf{k})$ in the k-space. The full expression of the coefficients $V_1(\ldots)$, $V_2(\ldots)$, $V_3(\ldots)$ and $W_4(\ldots)$ can be found in Zaslavskii and Polnikov (1998).

Usually Eq. (5) is used to derive the evolution equation for the statistical second moment of the normal canonical variable $b(\mathbf{k})$. For a spatial homogeneous wave field, the second moment is related to the wave action spectrum $N(\mathbf{k})$ by the formula

$$\langle b(\mathbf{k})b^*(\mathbf{k}')\rangle = N(\mathbf{k})\delta(\mathbf{k} - \mathbf{k}'), \tag{7}$$

where symbol $\langle\ldots\rangle$ means the theoretical ensemble averaging. Finally, the three-wave kinetic equation, which describe the time evolution of $N(\mathbf{k})$, can be expressed as (Davidson, 1972)

$$\frac{\partial N(\mathbf{k})}{\partial t} = 4\mathrm{Re}\left\{\int_0^t d\tau\int d\mathbf{k}_1\int Q(\mathbf{k},\mathbf{k}_1,\mathbf{k}_2,t,\tau)d\mathbf{k}_2\right\}. \tag{8}$$

where explicit dependence of $N(\mathbf{k})$ on time is omitted for simplicity, Re{...} is the real part of the expression in brackets, t is the evolution physical time and τ is the integrating time variable. Other symbols are as follows:

$$
\begin{aligned}
Q(\ldots) = {} & R_1(\mathbf{k},\mathbf{k}_1,\mathbf{k}_2,t')\exp[j\Delta\sigma(k,-k_1,-k_2)\tau] + \\
& + 0.5\, R_2(\mathbf{k},\mathbf{k}_1,\mathbf{k}_2,t')\exp[j\Delta\sigma(k,k_1,-k_2)\tau] + \\
& + R_3(\mathbf{k},\mathbf{k}_1,\mathbf{k}_2,t')\exp[j\Delta\sigma(k,k_1,k_2)\tau]
\end{aligned} \tag{9}
$$

where $t' = t-\tau$, and

$$\Delta\sigma(k, \pm k_1, \pm k_2) = \sigma(k) \pm \sigma(k_1) \pm \sigma(k_2) \tag{10}$$

$$
\begin{aligned}
R_i(\mathbf{k},\mathbf{k}_1,\mathbf{k}_2,t') = {} & [V_i^2(\mathbf{k},\mathbf{k}_1,\mathbf{k}_2)\delta(\mathbf{k} + s(1,i)\mathbf{k}_1 + s(2,i)\mathbf{k}_2)] \times \\
& \times N(\mathbf{k})N(\mathbf{k}_1)N(\mathbf{k}_2)\left[\frac{1}{N(\mathbf{k})} + \frac{s(1,i)}{N(\mathbf{k}_1)} + \frac{s(2,i)}{N(\mathbf{k}_2)}\right],
\end{aligned} \tag{11}
$$

$$s(1,1) = s(2,2) = s(2,1) = -1; \quad s(1,2) = s(1,3) = s(2,3) = 1. \tag{12}$$

Due to the oscillating feature of Q, the time integration of (8) is the main theoretical problem. Assuming the integral upper limit equal to infinity (i.e. assuming very slow nonlinear interaction), the integration of the harmonic component of Q results in (Davidson, 1972):

$$\mathrm{Re}\left\{\int_0^\infty \exp[j\Delta\sigma(k, \pm k_{1,} \pm k_2)\tau]d\tau\right\} \equiv \pi\delta[(k, \pm k_{1,} \pm k_2)]. \tag{13}$$

Due to impossibility to meet simultaneously the three-wave resonance conditions (1) and (2), the delta-functions in (11) and (13) result in

$$\partial N(\mathbf{k})/\partial t = 0 \tag{14}$$

(i.e. no evolution). Nevertheless, assuming a finite integral upper limit (i.e. $t = T_\beta(\mathbf{k})$, where $T_\beta(\mathbf{k})$ is the physical interaction time), Zaslavskii and Polnikov (1998) found:

$$
\begin{aligned}
\mathrm{Re}\left\{\int_0^{T_\beta(\mathrm{k})} \exp[j\Delta\sigma(k, \pm k_1, \pm k_2)\tau]d\tau\right\} &= \frac{\sin[T_\beta(\mathbf{k})\Delta\sigma(k, \pm k_1, \pm k_2)]}{\Delta\sigma(k, \pm k_1, \pm k_2)} \\
&= \pi\delta_\beta(\Delta\sigma(k, \pm k_1, \pm k_2))
\end{aligned} \tag{15}
$$

which is in fact a spread δ-function denoted hereinafter by the symbol $\delta_\beta(k, \pm k_1, \pm k_2)$. Unfortunately, due to its oscillating feature, the exact expression (15) of $\delta_\beta(k, \pm k_1, \pm k_2)$ cannot be used in practical computations. With the aim of finding a more regular approximation, the following identity can be used (e.g. Davidson, 1972):

$$\lim_{T\to\infty}\mathrm{Re}\left\{\int_0^T \exp[j\Delta\sigma\tau]d\tau\right\} = \lim_{\beta\to 0}\mathrm{Re}\left\{\frac{j}{\Delta\sigma + j\beta}\right\} = \lim_{\beta\to 0}\frac{\beta}{\Delta\sigma^2 + \beta^2}. \tag{16}$$

From a physical point of view, β in (16) represents a small attenuation of the wave amplitude with frequency $\Delta\sigma$ and it is therefore named attenuation parameter. Finally, the solution of the problem is found using (16) instead of (15). Therefore, the spread δ-function $\delta_\beta(k, \pm k_1, \pm k_2)$ is expressed as

$$\delta_\beta(k, \pm k_1, \pm k_2) = \frac{1}{\pi}\frac{\beta(\mathbf{k})}{[\Delta\sigma(k, \pm k_1, \pm k_2)]^2 + \beta^2(\mathbf{k})}, \tag{17}$$

and the evolution equation for the wave action spectrum becomes

$$\begin{aligned}\frac{\partial N(\mathbf{k})}{\partial t} &= 4\pi\int d\mathbf{k}_1\int\{V_1^2(\mathbf{k},\mathbf{k}_1,\mathbf{k}_2)\delta(\mathbf{k}-\mathbf{k}_1-\mathbf{k}_2)\delta_\beta(k,-k_1,-k_2)\times\\ &\times[N(\mathbf{k}_1)N(\mathbf{k}_2)-N(\mathbf{k})(N(\mathbf{k}_1)+N(\mathbf{k}_2))]-2V_1^2(\mathbf{k},\mathbf{k}_1,\mathbf{k}_2)\delta(\mathbf{k}_1-\mathbf{k}-\mathbf{k}_2)\times\\ &\times\delta_\beta(k_1,-k,-k_2)[N(\mathbf{k}_1)N(\mathbf{k})-N(\mathbf{k}_2)(N(\mathbf{k}_1)+N(\mathbf{k}))]\}d\mathbf{k}_2\end{aligned} \tag{18}$$

It must be noticed that $\beta(\mathbf{k})$ in (17) and (18) is the new theoretical function which describes the small attenuation of the wave amplitude due to the quasi-resonant three-wave interactions. In principal, $\beta(\mathbf{k})$ could be estimated as the inverse of the interaction time, i.e. $\beta(\mathbf{k})\cong 1/T_\beta(\mathbf{k})$, which is unfortunately not known apriori. With the aim of finding an alternative method of estimation, Zaslavskii and Polnikov (1998) proposed to rewrite (18) as:

$$\partial N(\mathbf{k})/\partial t = A(N)-B(N)N(\mathbf{k}), \tag{19}$$

where $A(N)$ and $B(N)$ are functions of the wave action density $N(\mathbf{k})$, obtained grouping positive and negative terms in r.h.s. of (18). The factor $B(N)$ in (19) can be considered as the rate of wave action decrease due to the nonlinearity. The main hypothesis of the theory consists in assuming $B(N)$ as the estimation for the unknown function $\beta(\mathbf{k})$, i.e.:

$$\begin{aligned}\beta(\mathbf{k}) = B(N) &= 4\pi\int d\mathbf{k}_1\int\Big\{V_1^2(\mathbf{k},\mathbf{k}_1,\mathbf{k}_2)\delta(\mathbf{k}-\mathbf{k}_1-\mathbf{k}_2)\delta_\beta(k,-k_1,-k_2)[N(\mathbf{k}_1)+N(\mathbf{k}_2)] +\\ &-2V_1^2(\mathbf{k},\mathbf{k}_1,\mathbf{k}_2)\delta(\mathbf{k}_1-\mathbf{k}-\mathbf{k}_2)\delta_\beta(k_1,-k,-k_2)[N(\mathbf{k}_2)-N(\mathbf{k}_1)]\Big\}d\mathbf{k}_2\end{aligned} \tag{20}$$

Solving iteratively (17) and (20) gives the function $\beta(\mathbf{k})$.

It must be stressed that the approximation proposed by Zaslavskii and Polnikov (1998) uses a couple of equations instead of one, as in the traditional theory.

System (18)-(20), which describes the wave action spectrum evolution in shallow water, was investigated both analytically and numerically by Polnikov (1998). In particular, the author studied the role of each integral term in (18) and the general features of the nonlinear spectral evolution $\partial N(\mathbf{k})/\partial t$ in the case of a homogeneous wave field propagating over constant depths. Among other results, it was found that the energy transfer depends essentially on the behavior of $\beta(\mathbf{k})$. The dependency of $\beta(\mathbf{k})$ on $\mathbf{k}$ was therefore investigated by varying the mean wave slope ϵ and the local depth h. In particular, it was found that the $\beta(\mathbf{k})$ grows almost linearly with the wave number $\mathbf{k}$ and the mean wave slope ϵ but it is inversely dependent on the local depth h, diminishing nearly to zero for values $k_p h \geq 1$.

3. Wave spectrum model

3.1. General equations

Preliminary computations based on a non stationary model have shown (Polnikov and Sychov, 1996) that the wave-field steady state is reached rather rapidly, i.e. in the time of peak wave propagation from the open-sea boundary to the shore. Therefore, the present work is based on a stationary spectral model of wave propagation.

The one-dimensional model used in our investigation is based on two equations: 1) the wave action evolution equation; 2) the momentum conservation equation. Such an approach to the description of the spectral evolution was originally proposed by Stive and Dingemans (1984) in the case of a single-component spectrum. In the present work this approach was extended to the full spectral representation.

The evolution equation for the wave action spectrum in a discrete representation ($N(\sigma_i)$) is expressed, in the case of no ambient currents and wave propagation normally to a parallel bottom contour, as:

$$\frac{\partial}{\partial x}\{N(\sigma_{\mathrm{i}})C_{\mathrm{g}}(\sigma_{\mathrm{i}})\} = NL(\sigma_{\mathrm{i}}) - Br(\sigma_{\mathrm{i}}), \tag{21}$$

where $C_g(\sigma_i)$ is the group velocity of the spectral component with frequency σ_i. $Br(\sigma_i)$ and $NL(\sigma_i)$ are the dissipation term due to wave breaking and the nonlinear term due to triad interactions, respectively. A description of both these terms is outlined for the discrete spectral representation in the next sub-sections.

The momentum conservation equation for free waves can be expressed, in the case of no ambient currents and wave propagation normally to a parallel bottom contour, as:

$$\frac{\partial S_{\mathrm{xx}}}{\partial x} + (h + \bar{\eta})\frac{\partial \bar{\eta}}{\partial x} = 0, \tag{22}$$

where h is the local depth, $\bar{\eta}$ is the mean level variation, and S_{xx} is the normal component of the radiation stress tensor ($\boldsymbol{S}$) in the x direction. In the linear approximation, the radiation stress component (S_{xx}) is expressed as:

$$S_{\mathrm{xx}} = \sum_{i=1}^{M}\left[\frac{C_{\mathrm{g}}(\sigma_{\mathrm{i}})}{C(\sigma_{\mathrm{i}})} - \frac{1}{2}\right]E(\sigma_{\mathrm{i}})\Delta\sigma, \tag{23}$$

where $C(\sigma_i)$ is the wave celerity of the spectral component, $\Delta\sigma = \sigma_{i+1} - \sigma_i$ is the spectral resolution, M is the number of spectral components, and $E(\sigma_i)$ is the wave energy spectral density, which is related to the wave action density by equation

$$E(\sigma_i) = N(\sigma_i)\sigma_i. \tag{24}$$

The solution method for Eqs. (21) and (22) is outlined in the subsection 3.4.

3.2. Nonlinear term

This term represents the rate of the wave action density transfer through the spectrum due to the quasi-resonant triad interactions (for each wave component and per unit area).

With the aim of introducing the three-wave quasi-kinetic approximation into the model, the general formulation of the nonlinear term [(18), (20)] has been simplified according to the considered situations. Assuming the shallow water condition ($kh < 1$) for all the spectral components, allows us to simplify the expression of the interacting coefficients $V_1(...)$, $V_2(...)$, $V_3(...)$ and $W_4(...)$. The quasi-kinetic system for a discrete one-dimensional wave action spectrum in the k-space is expressed, in the case of no ambient currents and wave propagation normally to a parallel bottom contour, as:

$$\begin{aligned} NL(k_i) = {} & \frac{9k_i g^{1/2}\Delta k}{32\pi h^{1/2}}\Bigl\{\sum_{j=1}^{i-1} k_j(k_i-k_j)\delta_\beta(k_i,k_j)[N_jN_{i-j}-N_i(N_j+N_{i-j})] + \\ & -2\sum_{j=i+1}^{M} k_j(k_j-k_i)\delta_\beta(k_i,k_j)[N_iN_{j-i}-N_j(N_i+N_{j-i})]\Bigr\}, \end{aligned} \tag{25}$$

where k_i, k_j and $|k_i-k_j|$ are the quasi-resonant three wave numbers, and

$$\delta_\beta(k_i,k_j) = \frac{1}{\pi}\frac{\beta(k_i)}{\Delta\sigma^2(k_i,k_j) + \beta^2(k_i)}. \tag{26}$$

In Eqs. (25) and (26) $\Delta\sigma(k_i, k_j)$ and $\beta(k_i)$ are given by

$$\Delta\sigma(k_i,k_j) = 0.5\sqrt{gh^5}|k_ik_j(k_i-k_j)|, \tag{27}$$

$$\begin{aligned} \beta(k_i) = {} & \frac{9k_i g^{1/2}\Delta k}{32\pi h^{1/2}}\Bigl\{\sum_{j=1}^{i-1} k_j(k_i-k_j)\delta_\beta(k_i,k_j)[N_j+N_{i-j}] + \\ & -2\sum_{j=i+1}^{M} k_j(k_j-k_i)\delta_\beta(k_i,k_j)[N_{j-i}-N_j]\Bigr\}. \end{aligned} \tag{28}$$

The wave number k_i is related to the frequency σ_i by the dispersion relation (4). Furthermore, the relationship between the wave-action density and the nonlinear term in the k-space and in the σ-space are expressed as:

$$N(k_i) = N(\sigma_i)C_g(\sigma_i), \tag{29}$$

$$NL(\sigma_i) = \frac{NL(k_i)}{C_g(\sigma_i)}. \tag{30}$$

The numerical method for the solution of the system (25)-(28) is presented in subsection 3.4.

3.3. Dissipation term

The dissipation of wave action density due to breaking, for each wave component and per unit area, can be expressed as:

$$Br(\sigma_{\mathrm{i}}) = W_{\mathrm{b}}N(\sigma_{\mathrm{i}}), \tag{31}$$

where

$$W_{\mathrm{b}} = \frac{\alpha}{\pi}\bar{\sigma}Q_{\mathrm{b}}\frac{H_{\mathrm{lim}}^2}{H_{\mathrm{rms}}^2}, \tag{32}$$

Eq. (31) is similar to that originally proposed by Eldeberky and Battjes (1996), who elaborated the Battjes and Janssen (1978) theory about the dissipation of monochromatic wave energy due to breaking. While in the Battjes and Janssen formulation W_b has the physical meaning of the wave-energy fraction dissipated by breaking, in the present work W_b represents the fraction of the total wave action dissipated due to breaking, for the reason of the linear relation between the wave energy and the wave action.

In (32) α is the fitting coefficient (typical value $\alpha = 1$), $\bar{\sigma}$ is the mean spectral frequency, Q_b is the breaking probability, H_{rms} is the root mean square height and H_{lim} is the maximum non-breaking wave height. The definitions of $\bar{\sigma}$ and H_{rms} are as follows

$$\bar{\sigma} = \sqrt{\sum_{i=1}^{\mathrm{M}} \sigma_{\mathrm{i}}^3 N(\sigma_{\mathrm{i}}) / \sum_{i=1}^{\mathrm{M}} \sigma_{\mathrm{i}} N(\sigma_{\mathrm{i}})}, \tag{33}$$

$$H_{\mathrm{rms}} = \sqrt{8\sum_{i=1}^{\mathrm{M}} \sigma_{\mathrm{i}} N(\sigma_{\mathrm{i}})\Delta\sigma}, \tag{34}$$

The value of H_{lim} is computed by Miche's criterion of the following kind (Stive and Dingemans, 1984)

$$H_{\mathrm{lim}} = \frac{2\pi\gamma_{\mathrm{d}}}{\bar{k}}\tanh\left(\frac{\gamma_{\mathrm{s}}}{2\pi\gamma_{\mathrm{d}}}\bar{k}h\right), \tag{35}$$

where $\bar{k}$ is the wave number corresponding to $\bar{\sigma}$, γ_d is the deep water breaking coefficient (typical value $\gamma_d = 0.14$) and γ_s is the shallow water breaking coefficient (typical value $\gamma_s = 0.8$).

For a fixed water depth, Q_b is the fraction of waves exceeding the limiting wave height (H_{lim}) and can be calculated using the following statistical relation derived by Battjes and Janssen (1978):

$$\ln Q_{\mathrm{b}} = (Q_{\mathrm{b}} - 1)\frac{H_{\mathrm{lim}}^2}{H_{\mathrm{rms}}^2}. \tag{36}$$

It should be noted that (31) implies that the proposed mechanism for the wave breaking does not change the spectral shape but causes only a proportional reduction of wave action density for each wave component. The reliability of this assumption was proved by Eldeberky and Battjes (1996) using numerical simulations.

3.4. Numerical method

The numerical solution of Eqs. (21) and (22), which are discretized over an uniform grid, is based on the space marching fourth order Runge–Kutta method.

Firstly, the normal component of the radiation stress tensor in the x direction (S_{xx}) is computed using (23). Secondly, the mean water level variation is calculated solving (22), and the local depth is up-dated correspondingly. Furthermore, once the nonlinear and the dissipative terms are properly evaluated, Eq. (21) can be solved.

The system (25)-(28) must be solved to compute the nonlinear term. Assuming

$$\beta(k_{\mathrm{i}})_0 = 0.1\sigma_{\mathrm{i}} \tag{37}$$

as guess value makes it possible to solve (25). Afterwards, the system (25)-(28) is iteratively solved till the convergence condition

$$|\beta(k_{\mathrm{i}})_{\mathrm{n}} - \beta(k_{\mathrm{i}})_{\mathrm{n-1}}| < \xi\beta(k_{\mathrm{i}})_{\mathrm{n}} \tag{38}$$

is met (n is the iteration index). Some numerical tests have shown that, if ξ is less than 0.1, the choice of ξ doesn't remarkably influence the solution of the system. It should be noticed that when $\xi = 0.1$ three or four iterations are sufficient to satisfy the convergence condition (38). Substituting $\beta(k_i)_n$ into (25) makes it possible to calculate the nonlinear term in k-space ($NL(k_i)$). Finally, the nonlinear term $NL(k_i)$ is related to the nonlinear term in σ-space ($NL(\sigma_i)$) by (30).

Using (33) and (34) is possible to compute $\bar{\sigma}$ and H_{rms} and therefore the breaking term. The mean wave number $\underline{k}$ results from the dispersion relation (4). The maximum limiting wave height (H_{lim}) is computed by Miche's criterion (35) and the parameter Q_b is found solving iteratively (36). Substituting all these values into (32), the wave-action density dissipated by breaking is found using (31).

After (21) is solved, the solution of the problem advances in space.

4. Method of investigation

The wave evolution in shallow water is determined mainly by the following physical phenomena: shoaling, refraction, nonlinear interactions and breaking. The combination of these phenomena makes the experimental investigation of each evolution mechanism rather complicated. Nevertheless, in numerical experiments, it is possible to separate each effect by choosing the simplest physical situation and the related expression for the source function in the r.h.s. of (21).

In the present paper waves are considered propagating from the open boundary normally to the shore, which makes possible to neglect the refraction effect leaving its analysis for further study.

Aiming to validate the three-wave quasi-kinetic approximation, at first some simple test simulations, without invoking any experimental data, was considered. The results obtained in these simulations were in fact analyzed on the basis of general physical considerations, with the particular aim of pointing out the role of each evolution mechanism. Once the influence of each phenomenon on the spectral evolution was clarified, the numerical results were compared to the experimental measurements obtained by Arcilla et al. (1994) and Beji and Battjes (1993).

The results of the numerical tests are presented in the next section while the validation is presented in the section six. The analysis of the results are carried out in terms of the following spectral characteristics:

1. two integral parameters;
2. shape ($E(\sigma_i)$).

The integral parameters taken into account are the root mean square height (H_{rms}), given by (34), and the mean period (T_m) defined as

$$T_m = \frac{2\pi}{\bar{\sigma}}, \tag{39}$$

where $\bar{\sigma}$ is given by (33).

The use of wave energy spectrum ($E(\sigma_i)$) instead of wave action one ($N(\sigma_i)$) is provided by standard measurements of energy spectrum “in situ”. Transition from $E(\sigma_i)$ to $N(\sigma_i)$ and to $N(k_i)$ is governed by relations (24) and (29).

5. Results of numerical testing

The test simulations were carried out in order to understand the role of three-wave non resonant interactions and breaking in the wave spectrum evolution in shallow water (i.e. when $k_p h < 1$). In order to separate the effect of shoaling, the following two situations are considered:

- a) constant depth (no shoaling, the nonlinear and breaking effects are present);
- b) constant bottom slope (all the mechanisms occur).

In all the tests, the 1D axis of propagation is 100 m long and is discretized in 101 points ($\Delta x = 1$ m). The shape of the initial spectrum is given by the JONSWAP parameterization

$$E(\sigma) = C\sigma^{-5}g^2\exp\left[-1.25\left(\frac{\sigma_p}{\sigma}\right)^5\right]\gamma^{\exp\left[\frac{(\sigma-\sigma_p)^2}{0.01\sigma^2}\right]}, \tag{40}$$

where C is the Philips coefficient, σ_p is the peak frequency and γ is the peak enhancement coefficient. For all the testing simulations carried out, these parameters had the following values: $C = 0.0005$, $\sigma_p = 0.785\ rad/s$ ($f_p = 0.125\ Hz$), $\gamma = 3.4$, $H_{rms} = 0.43$ m.

The numerical results are considered at six fixed spatial points distributed uniformly (every 20 m) from the outer boundary to the shore.

5.1. Constant depth case

The water depth is taken equal to $h = 2$ m (i.e. $k_p h = 0.36$ and $H_{lim}/H_{rms} \approx 4$). The principal results are presented in Fig. 1, where the spectral shape E(σ) at the six locations is depicted in the case in which only the nonlinear term is included in the *r.h.s* of (21). The figure shows that secondary peaks at multiple frequencies (double and triple of σ_p) are obtained. A significant increase of spectral energy at frequencies higher than σ_p and a significant decrease of spectral density in a band centered on σ_p characterize the evolution of the spectrum. This behavior is typical of the spectral shape observed experimentally by Freilich and Guza (1984). On the basis of this result, it can be definitely concluded that the triad nonlinear interaction provides energy transfer from the band centered on the primary peak to the upper frequencies (super-harmonics).

5.2. Constant slope case

A weakly sloped depth profile [$h(x) = 2.0–0.01x$, $0 \le x \le 100$ m, $0.25 \le k_p h \le 0.36$] was considered. The spectral shape evolution is presented in Fig. 2, in which four cases are shown, corresponding to the following model configuration:

a) pure shoaling (no source terms are included in the r.h.s. of (21));
b) shoaling and nonlinear interactions (the breaking term is excluded);

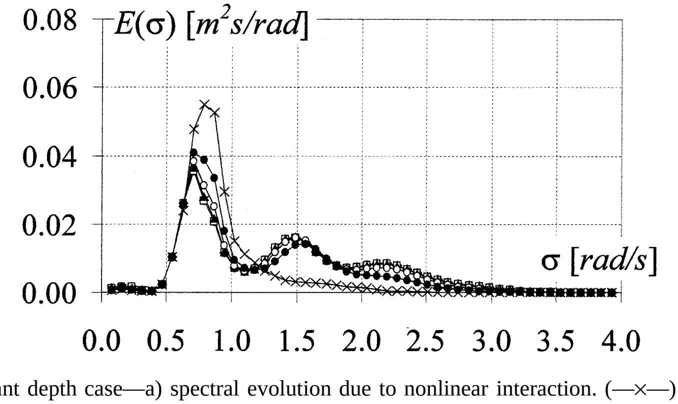

Fig. 1. Constant depth case—a) spectral evolution due to nonlinear interaction. (—×—) boundary condition (JONSWAP spectrum; $C = 0.0005$, $\sigma_p = 0.785\ rad/s$, $\gamma = 3.4$, $H_{rms} = 0.43$ m); (—●—) station 2 at 20 m from open-sea; (—○—) station 3 at 40 m from open-sea; (—▲—) station 4 at 60 m from open-sea; (—□—) station 5 at 80 m from open-sea; (—◆—) station 6 at 100 m from open-sea.

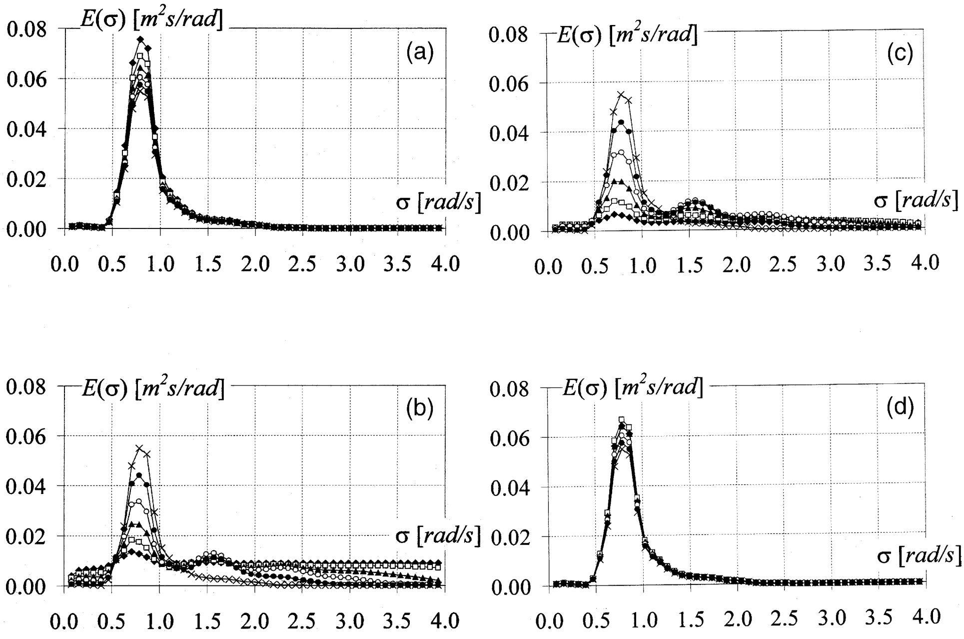

Fig. 2. Constant slope case–a) spectral evolution due to shoaling; b) spectral evolution due to nonlinear interaction and shoaling; c) spectral evolution due to nonlinear interaction, shoaling and breaking; d) spectral evolution due to shoaling and breaking. For other notations see legend of Fig. 1.

c) shoaling, breaking and nonlinear interactions (all terms are included);
d) shoaling and breaking (the nonlinear term is excluded).

The result obtained in the first case (Fig. 2a) shows a rather strong shoaling (~50%) without remarkable change of the peak frequency. This is a typical test to check the numerical scheme.

In the second case (Fig. 2b), the result shows the combined effect of nonlinearity and shoaling. It should be noticed that the shoaling effect on the peak-side-band components is completely suppressed by the nonlinear interactions. The secondary peaks are visible only at small distances from the outer boundary (i.e. for a short evolution time) while an unrealistic white noise spectrum is obtained at large distances.

In the third case (Fig. 2c), the secondary peaks due to nonlinear interactions are conserved for all the evolution time, but with different amplitudes. Under these conditions, the energy traveling with the secondary peaks is still remarkable. Fig. 2d illustrates the evolution of a wave spectrum without nonlinear term. The figure shows the absolute absence of secondary peaks. It must be noted that while the shoaling is only reduced by the breaking term when $k_p h > 0.3$, it is completely suppressed when $k_p h < 0.3$.

It should also be noticed that during the propagation (Fig. 3a), whilst T_m (39) decreases radically (about 55%), H_{rms} (34) is reduced to about 30% of its maximum value when both nonlinear and breaking terms are included in the r.h.s. (21). The mean period evolution is clearly related to nonlinear interactions. Herewith, the H_{rms} evolution is not determined only by breaking. The exclusion of the nonlinear term from the computation leads in fact to an H_{rms} reduction of 2% of its maximum value (Fig. 3b).

In the present case, nonlinearity influences severely the breaking dissipation intensity. From a physical point of view, this effect can be interpreted considering the energy transfer from the non breaking long wave to the intensively breaking short wave produced by the nonlinear interactions.

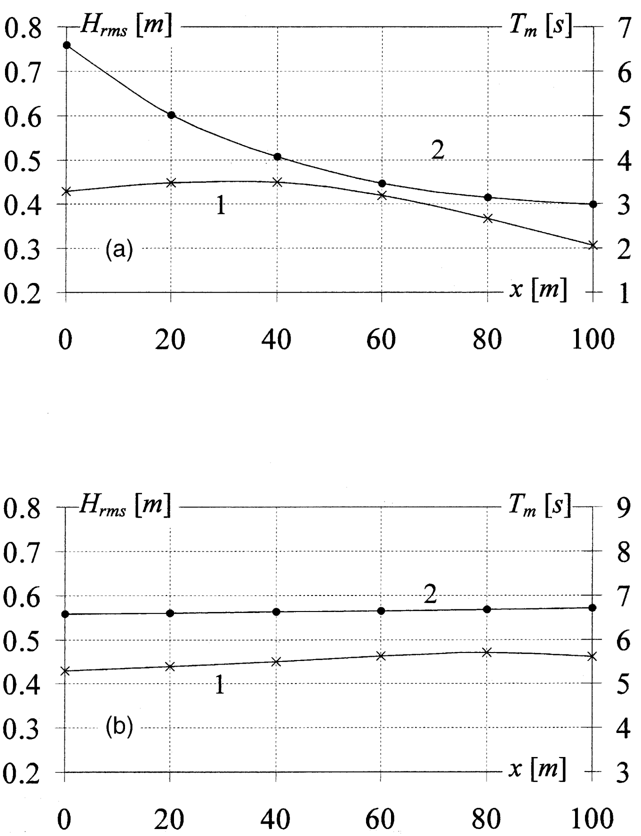

Fig. 3. Constant slope case—(1) H_{rms} (–×–) and (2) T_m (—●—): a) evolution due to nonlinear interaction, shoaling and breaking (the relative spectral shape evolution is shown in Fig. 2c); b) evolution due to shoaling and breaking (the relative spectral shape evolution is shown in Fig. 2d).

6. Validation of the three-wave quasi-kinetic approximation

In order to validate the three-wave quasi-kinetic approximation for spectral evolution in shallow water, the numerical model has been applied to the tests carried out by Arcilla et al. (1994) and by Beji and Battjes (1993).

It must be noticed that the breaking term has first been calibrated in order to select the values of γ_d and γ_s which give the best agreement between the numerical and observed space evolution of T_m and H_{rms} [(39), (34)].

6.1. Experiment of Arcilla et al. (1994)

Fig. 4 illustrates both the depth profile and the location of the wave recording station reproduced in the numerical test, in which the relative depth parameter varies between $0.29 < k_p h < 0.53$. The breaking coefficients, determined during the calibration, are: $\gamma_d = 0.12$ and $\gamma_s = 0.64$. The input spectral shape, which has been digitized from that presented in the original paper, is characterized by a very narrow energy distribution around the peak frequency ($\sigma_p = 0.785\,rad/s$), with $H_{rms} =$ 0.43 m.

First and foremost, we note the features of the bottom topography (see Fig. 4) and try to foretell the expected spectral evolution. The wave-spectrum evolution induced by the depth profile can be divided into two different stages. In the first stage, the wave motion, characterized by a very narrow spectrum, is incident on a rather steep bottom slope (about 1:20), small in length. In principle, this situation must lead to a marked shoaling effect and a weak nonlinear interaction (due to the short interaction time). In the second stage, the bottom slope is mild (about 1:70). Now, the expected contributions of the shoaling and nonlinearity effects must be interchanged.

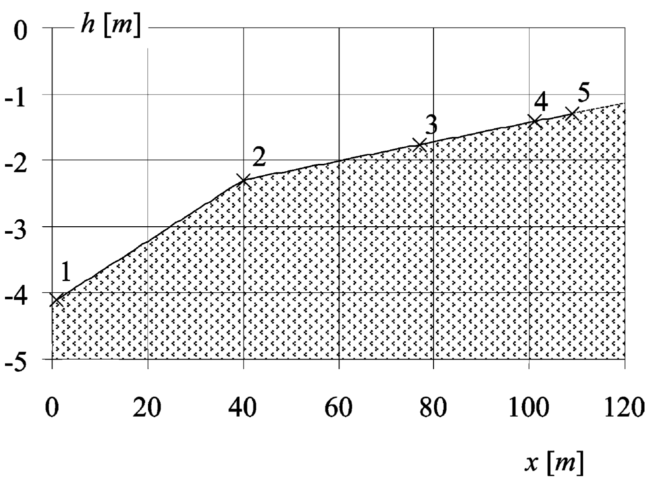

Fig. 4. Depth profile and recording stations distribution used in the experiment of Arcilla et al. (1994).

The evolution of both the computed and observed H_{rms} and T_m are shown in Fig. 5, while Fig. 6 shows the comparison between the shapes of the spectrum calculated using the numerical model, and those reported in the original paper. It must be noticed that both integral characteristics and spectral shapes show good agreement, although a small discrepancy between the primary peak intensities takes place at the final stage of evolution (Figs. 6d and 6e).

The obtained discrepancy at stations n°4 and 5 (see Figs. 6d and 6e) might be explained as follows. On the one hand, it is necessary to take into account the confidence intervals of the observed spectra, which are not presented in Arcilla et al. (1994). On the other hand, since the density energy distribution in the high frequency band is slightly overestimated it is possible to assume that the nonlinear term works too intensively for $k_p h \approx 0.3$. This assumption can be strengthened by comparing the numerical and experimental evolutions of H_{rms} and T_m at station n° 4 and 5 (see Fig. 5). The computed T_m is in fact underestimated by about 1 s while the computed H_{rms} is practically coincident with the measured one.

6.2. Experiment of Beji and Battjes (1993)

Fig. 7 illustrates both the depth profile and the location of the wave recording station reproduced in the numerical test, in which the relative depth parameter varies between $0.28 < k_p h < 0.6$. The bar profile is characterized by an offshore slope of 1:200 and an inshore slope of 1:100. The breaking coefficients, determined during the calibration step, are: $\gamma_d = 0.12$ and $\gamma_s = 0.64$. The input spectral shape, which has been digitized from that presented in the original paper, is characterized by a very narrow energy distribution around the peak frequency ($\sigma_p = 2.827\ rad/s$), and by $H_{rms} = 0.017$ m.

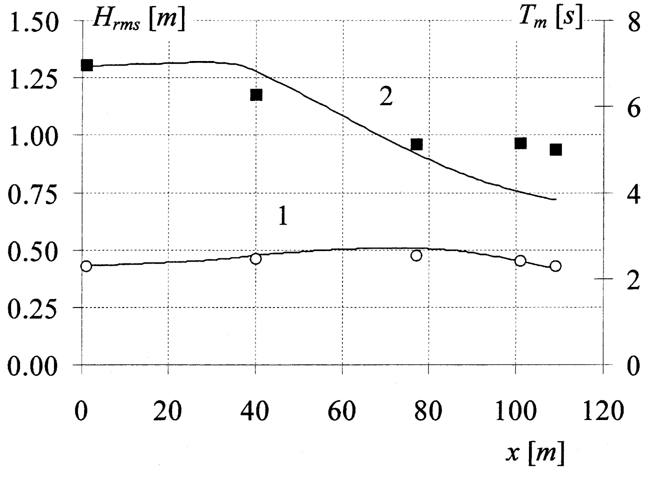

Fig. 5. Arcilla et al. experiment (1994)—model calibration. (1) Root mean square wave height (○ observed, — computed) and (2) mean period (■observed, — computed).

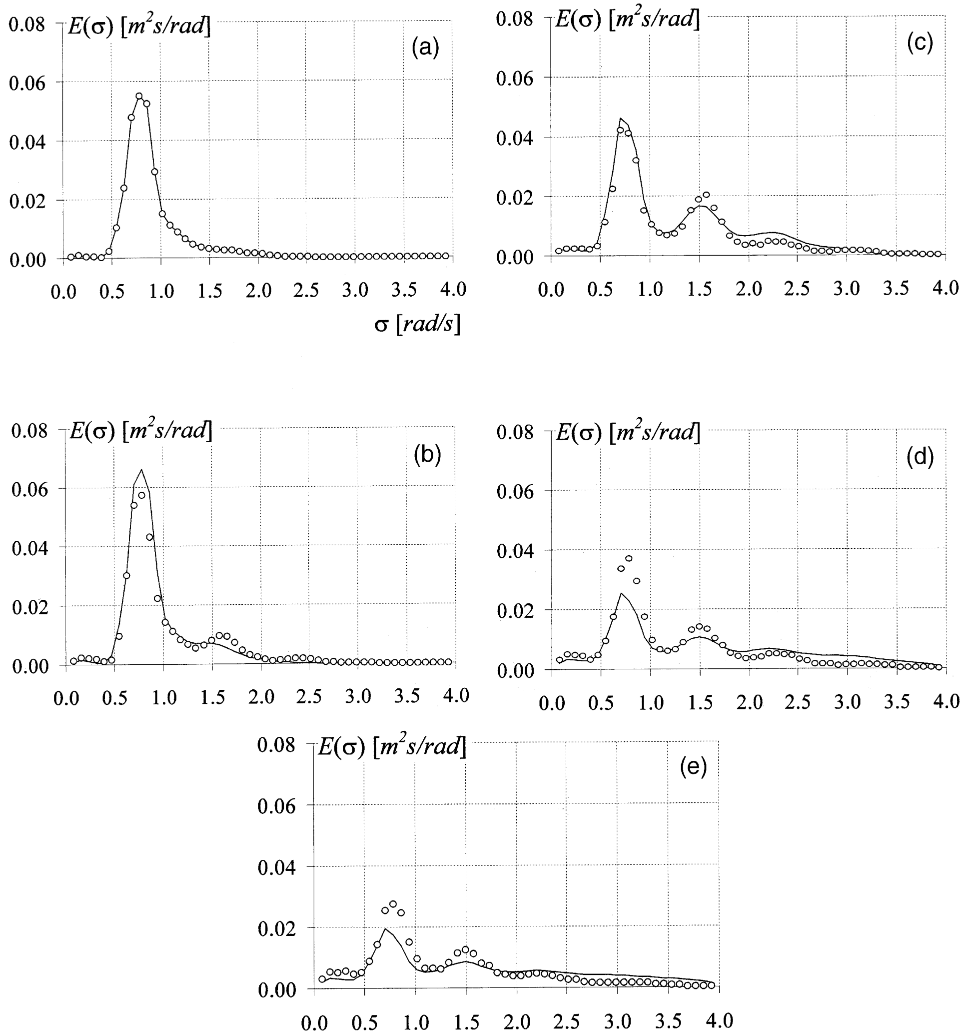

Fig. 6. Arcilla et al. experiment (1994)—spectral shape evolution. Comparison of the numerical results (—) against the observed data (○). *a*) open-sea boundary condition - recording station 1; *b*) recording station 2; *c*) recording station 3; *d*) recording station 4; *e*) recording station 5;

The evolution of both the computed and observed H_{rms} and T_m are shown in Fig. 8, which shows very good agreement, while Fig. 9 shows the comparison between the shapes of the spectrum calculated using the numerical model and those reported in the original paper. It must be noticed that the shoaling effect is particularly evident in this experiment. In the first stage of wave propagation, H_{rms} significantly increases and T_m slightly decreases (see Fig. 8). It must be noticed that, in this case, H_{lim} corresponding to the lower depth at the top of the bar is about three times greater that H_{rms} (H_{lim} = 0.064 m and H_{rms} = 0.023 m). Over the bar, no breaking and no

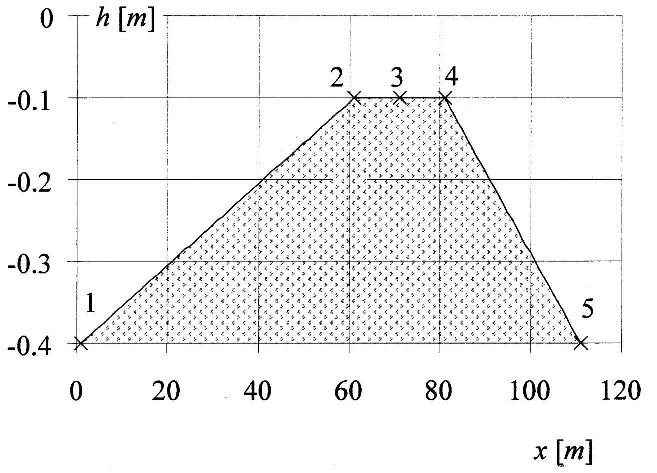

Fig. 7. Depth profile and recording stations distribution used in the experiment of Beji and Battjes (1993).

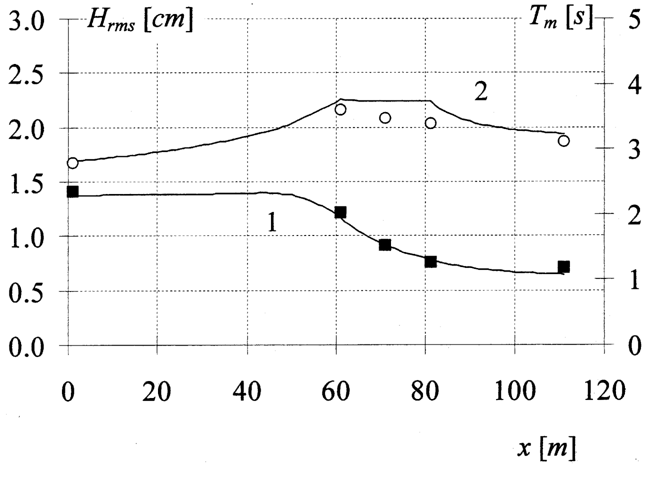

Fig. 8. Beji and Battjes experiment (1993)—model calibration. For other notations see legend of Fig. 5.

shoaling occur but intense nonlinear interaction is evident. After the bar, neither breaking nor nonlinear interaction modify the shape of the spectrum.

The spectral shape evolution is shown in Fig. 9. As can be seen, the computed spectral shapes agree with the observed ones, although the secondary peaks are underestimated at final stations.

It should be noted that this experiment was treated in detail in Eldeberky and Battjes (1996). Using a phase-resolving wave model with special fitting parameters for the triads interaction term, these authors found the numerical spectral evolution in good agreement with the experimental data. In the present work the same agreement was obtained without any fitting parameter for the nonlinear term. This feature

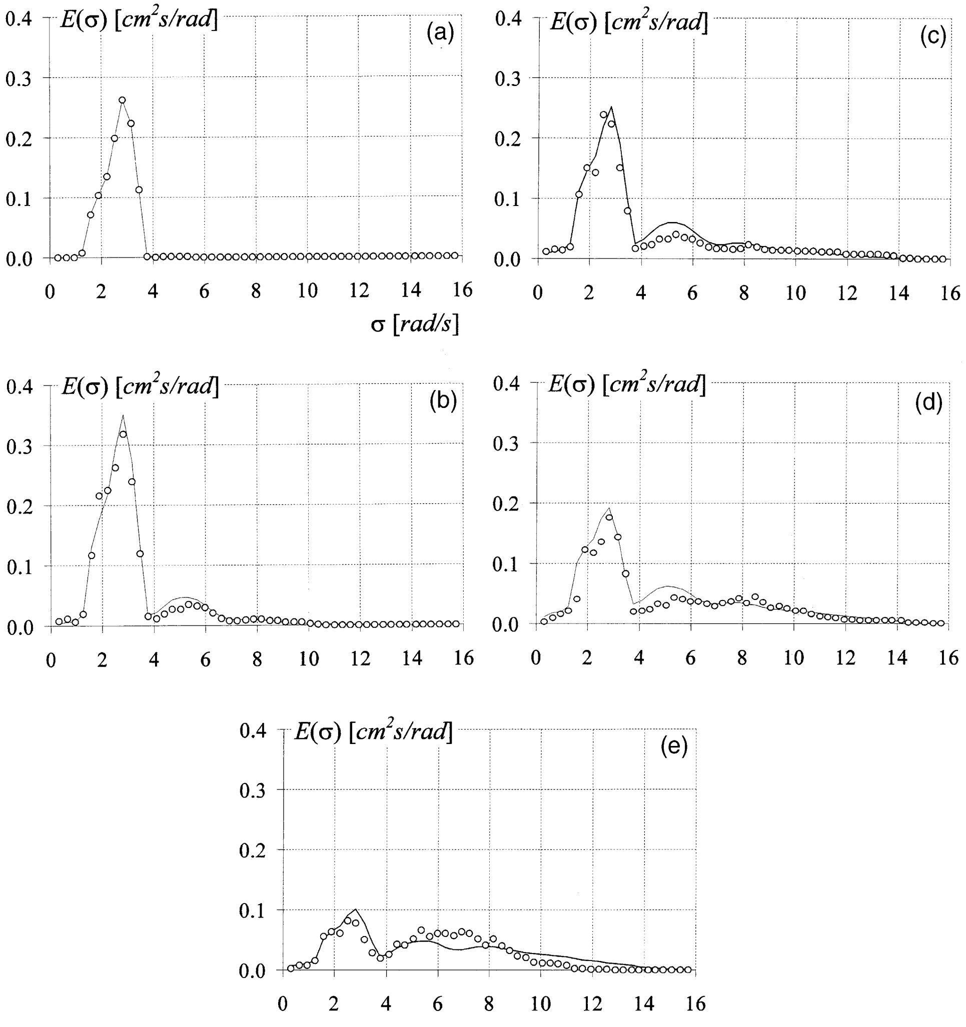

Fig. 9. Beji and Battjes experiment (1993)—spectral shape evolution. For other notations see legend of Fig. 6.

is the main advantage of the quasi-kinetic approximation used in the present work to reproduce the nonlinear interaction effect.

7. Conclusions

The present work was aimed to validate the three-wave quasi-kinetic approximation for the nonlinear interaction in shallow water, using specific test for unidirectional waves. A spectral model that adequately reproduces all the main features in the evolution of the shallow-water wave spectrum is developed. The nonlinear term based on the Zaslavskii and Polnikov (1998) three-wave quasi-kinetic approximation is found to be of considerable importance in this model. Additionally it is shown that the breaking term proposed by Battjes and Janssen (1978), expressed in the spectral representation by Eldeberky and Battjes (1996), also plays a very significant role.

The computations performed give a clear idea of the contributions made by different physical processes to the evolution of the wave spectrum in shallow-water. It is shown that three-wave non-resonant nonlinear interactions can be used to simulate the wave energy transfer from the fundamental harmonic to higher frequencies, with the formation of peaks at multiple frequencies. In terms of integral wave characteristics, the nonlinear effect is responsible for a significant decrease in the mean wave period T_m. However, this decrease is generally not accompanied by a significant change in the root mean square wave height. But when breaking occurs, the nonlinear interactions increase the energy dissipation rate, transferring energy from long non breaking waves trough short breaking waves. Moreover, it is found that the Battjes–Janssen breaking mechanism adequately describes the effect of shoaling compensation and the formation of the high-frequency tail of the spectrum.

The problem of joining the four-wave nonlinear approximation, which is valid in deep water ($k_p h > 1$), and the three-wave non-resonant approximation, which is effective in shallow water ($k_p h < 1$), calls for further study.

Acknowledgements

Authors are grateful to Prof. Noli for the organizing of the joint study and to the Administration of the Rome University ‘La Sarienza’ for the financial support for Prof. V. Polnikov visiting the Civil Engineering Department of the University.

References

Abreu, M., Larraza, A., Thornton, E., 1992. Nonlinear transformation of directional wave spectra in shallow water. J. Geophys. Res. 97C, 15579–15589.

Arcilla, A.S., Roelvink, B.A., O’Connor, A.J.H.M., et al., 1994. The Delta Flume ‘93 Experiment. Proc. Coastal Dynamics Conf.’94, Barcelona, Spain, pp. 488–502.

Battjes, J.A., Janssen, J.P.F.M., 1978. Energy loss and set-up due to breaking of random waves. Proc. 16th Int. Conf. On Coastal Eng., pp. 569–587.

Beji, S., Battjes, J.A., 1993. Experimental investigation of wave propagation over a bar. Coastal Eng 19, 151–162.

Beji, S., Nadaoka, K., 1997. Spectral modelling of nonlinear shoaling and breaking over arbitrary depths. Proc. Coastal Dynamics ‘97, pp. 285–300.

Beji, S., Nadaoka, K., 1999. A spectral model for unidirectional nonlinear wave propagation over arbitrary depths. Coastal Eng 36, 1–16.

Crawford, D.R., Saffman, P.G., Yuen, H.C., 1980. Evolution of a random inhomogeneous field of nonlinear deep-water gravity waves. J. Wave Motion. 2, 1–16.

Davidson, R.C., 1972. Weak turbulence theory of nonlinear wave-wave interactions. In: Methods in nonlinear plasma theory. Academic Press, New York & London, pp. 243–273.

Eldeberky, Y., Battjes, Y., 1996. Spectral modelling of wave breaking: application to Boussinesq equation. J. Geophys. Res. 101 (C1), 1253–1264.
Elgar, S., Guza, R.T., 1986. Non-linear model predictions of bispectra of shoaling surface gravity waves. J. Fluid Mech 167, 1–18.
Freilich, M.H., Guza, R.T., 1984. Non-linear effects on shoaling surface gravity waves. Phil. Trans. Royal Soc. London, A 311, 1–41.
Hasselmann, K., 1962. On the non-linear energy transfer in a gravity wave spectrum. Pt. 1. J. Fluid Mech. 12, 481–500.
Hasselmann, K., Ross, D.B., Muller, P., Sell, W.A., 1976. Parametric wave prediction model. J. Phys. Oceanogr. 6 (2), 200–228.
Holthuijensen, L.H., Booij, N., Ris, R.C., 1993. A spectral wave model for the coastal zone. In: Magoon, O.T., Hemsley, J.M. (Eds.), Ocean Wave Measurement and Analysis. ASCE, pp. 613–641.
Madsen, P.A., Sørensen, O.R., 1992. A new form of the Boussinesq equations with improved linear dispersion characteristics. Pt. 2: a slowly-varying bathymetry. Coastal Eng. 18, 183–205.
Madsen, P.A., Sørensen, O.R., 1993. Bound waves and triad interactions in shallow water. J. Ocean Eng. 20 (4), 359–388.
Nwogu, O., 1994. Non-linear Evolution of Directional Wave Spectra in Shallow Water. Proc. Coastal Eng. Conf. 24th, pp. 447–481.
Peregrine, D.H., 1967. Long waves on a beach. J. Fluid Mech. 27, 815–827.
Phillips, O.M., 1960. On the dynamics of unsteady gravity waves of finite amplitude. Pt. 1. J. Fluid Mech. 9, 193–217.
Polnikov, V.G., Sychov, E.N., 1996. On a numerical modeling of a wave spectrum evolution for shallow water. Oceanology 36 (6), 827–834 in Russian.
Polnikov, V.G., 1998. A study of the three-wave quasi-kinetic approximation equations for nonlinear gravity waves in a finite depth water. Izv., Atmospheric and Ocean Phys. 34 (6), 757–764 English translation.
Resio, D.T., 1988. A steady-state Wave Model for Coastal Applications. Proc. Coastal Eng. Conf. 21st, pp. 929–940.
Stive, M., Dingemans, M., 1984. Calibration and Verification of a One Dimensional Wave Energy Decay model. Report on investigation, T.O.W.
Young, I.R., Van Vledder, G.Ph., 1993. The central role of non-linear interactions in wind–wave evolution. Phil. Trans. Royal Soc. L. A 342, 505–524.
Zakharov, V.E., 1974. Hamiltonian formalism for waves in the non-linear media with dispersion. Izv. VUZov, scr. Radiophysica 17 (4), 431–453.
Zakharov, V.E., 1998. Weakly nonlinear waves on the surface of an ideal finite depth fluid. Amer. Math. Soc. Trans 182 (2), 167–197.
Zaslavskii, M.M., Krasitskii, V. P., Gavrilin, B.L., 1995. Shallow Water Limitations for Application of the Four-wave Interactions of Nonlinear waves in the Finite Depth Water. Proc. Conf. Dynamics of Ocean and Atmosphere. Moscow, November 22–25, p. 139.
Zaslavskii, M.M., Polnikov, V.G., 1998. Three-wave quasi-kinetic approximation in the problem of non-linear gravity wave spectrum evolution in water of finite depth. Izv., Atmospheric and Ocean Phys. 34 (5), 609–616 English translation.